Progress in Superconductivity Vol.3 No.1 pp65-69 31 October 2001

# Transport Properties of Ramp-Edge Junction with Columnar Defects

C. W. Lee [a], D. H. Kim*, [a], T. W. Lee [a], Gun Yong Sung [b], Sang Hyeob Kim [b], JunHo Kim [b], T. S. Hahn [c]

[a] *Institute of Basic Sciences, Yeungnam University, Kyungsan, Korea*
[b] *Electronics and Telecommunications Research Institute, Taejon, Korea*
[c] *Korea Institute of Science and Technology, Seoul, Korea*

Received 20 August 2001

# 원통형 결함을 포함한 Ramp-Edge Junction의 수송특성

이창우[a], 김동호*, [a], 이태원 [a], 성건용 [b], 김상협 [b], 김준호 [b], 한택상 [c]

**Abstract**

We measured the transport properties of $YBa_2Cu_3O_x$ ramp-edge junction fabricated with interface-engineered barrier. The current-voltage characteristics show a typical resistively-shunted junction like behavior. Voltage noise measurement revealed that the main source of the $1/f$ noise is the critical current and resistance fluctuations. The analysis of the noise data showed that the critical current fluctuations increase with temperature, whereas the resistance fluctuations are almost constant, and both fluctuations are antiphase correlated. The smaller magnitude of the critical current and resistance fluctuations seems to result from the columnar-defects.

*Keywords*: Ramp-edge junction, $1/f$ noise, critical current and resistance fluctuations

## I. Introduction

High temperature superconducting (HTS) Josephson junctions are important elements for the superconducting device applications. Many types of high-$T_c$ Josephson junctions have been fabricated such as grain boundary junctions, step-edge junctions, superconductor/interface/superconductor ramp-edge junctions, and e-beam written junctions. Still HTS junctions are not yet commercially ready when compared with their low-$T_c$ counterparts. The inherent limits of these junctions are from the intrinsic properties of HTS materials such as a very short coherence length and large thermal fluctuations due to their high operating temperatures. The complicated morphology associated with the growth mechanism of HTS thin films is another limitation that should be controlled prior to commercial applications.

Recently, Moeckly *et al.* [1] created uniform and

*Corresponding author. Fax: +82 53 814 6141
e-mail: dhkim@yu.ac.kr

reproducible $YBa_2Cu_3O_x$ (YBCO) thin film ramp-edge junctions by a interface-engineered junction technique. Here the barrier is formed on a ramp-edge surface of the YBCO base electrode by structural modification using *in-situ* plasma treatment prior to deposition of the YBCO counter electrode.

One useful method to study the nature of the charge transport across the barrier in HTS Josephson junctions is voltage noise measurement. Low frequency $1/f$ noise properties have been employed to understand the weak-link nature of the barrier in YBCO bicrystal grain-boundary junctions, biepitaxial grain-boundary junctions and SNS ramp-edge junctions. Kawasaki *et al.* [2] explained $1/f$ noise of YBCO bicrystal grain-boundary junctions assuming two sources of fluctuations, critical current and resistance fluctuations. Marx *et al.* [3] measured $1/f$ noise of $Bi_2Sr_2CaCu_2O_{8+x}$ (Bi-2212) bicrystal grain-boundary junctions. The origin of $1/f$ noise is shown to be critical current and resistance fluctuations as well.

The voltage noises of ramp-edge SNS junctions are also reported. Myers *et al.* [4] measured $YBCO/CaRuO_3/YBCO$ junctions and interpreted that $1/f$ noise is a result of the distribution of life times of carriers trapped in different types of interface regions with different electrical properties. Flett *et al.* [5] reported voltage noise properties of YBCO/Co-YBCO/YBCO junctions. On the other hand, no voltage noise study has been yet reported on interface-engineered ramp-edge junctions. In this paper we present current-voltage (*I-V*) characteristics and voltage noise measurement in interface-engineered ramp-edge junction.

## II. Experiments

The fabrication process for interface-engineered ramp-edge junctions is based on a two-step ion milling process, in which the etching mask is a patterned $Sr_2AlTaO_6$ (SAT) layer on the YBCO base electrode. The detailed process is described elsewhere [6]. 200-nm thick YBCO was grown by KrF pulsed laser deposition (PLD) on a $LaAlO_3$ (100) single crystal substrate. The ramp edge was damaged by high voltage argon-ion beam of 700 V to form the junction barrier. Following the ion-beam damage, we annealed the samples at 500 °C under oxygen atmosphere of 400 mtorr for 30 min and deposited the YBCO counter electrode and SAT by PLD. The vacuum annealing was necessary to transform the ion-beam damaged layer to a stable and resistive barrier. Finally, Au was deposited and patterned by lift-off for the contact.

Then, the junctions were irradiated by 1.3-GeV Pb ions at Argonne Tandem Linear Accelerator System. The dose, ~2 x $10^{10}$ defects/cm$^2$, is equivalent to the vortex density of 4 kG. The average number of the defects piercing the barrier is ~500 for 5-μm wide junction. The orientation of columnar defects is roughly along the *c* axis of the both YBCO electrodes. The junctions were placed inside a single-wall mu-metal shield during the measurement. It has been shown [7] that both the critical current $I_c$ and $I_cR_n$, the product with the normal-state resistance $R_n$, increase after introducing columnar defects.

## III. Results and Discussions

The resistive transition of 5-μm wide is shown in Fig. 1. The YBCO electrodes become superconducting below 90 K and the junction becomes fully superconducting below 84 K. The expanded view of the resistive tail is shown in the inset. Also shown is the temperature dependence of $R_n$ of the junction that is determined from *I-V*

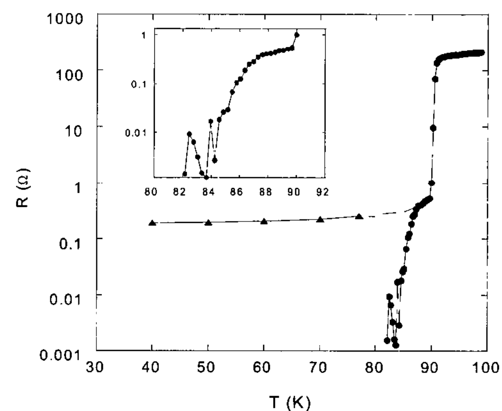


Fig. 1. The resistive transition of 5-μm wide is shown. The inset shows an expanded view of the resistive tail. Triangles are $R_n$ that slightly decreases with temperature from 0.26 Ω at 77 K to 0.19 Ω at 30 K.

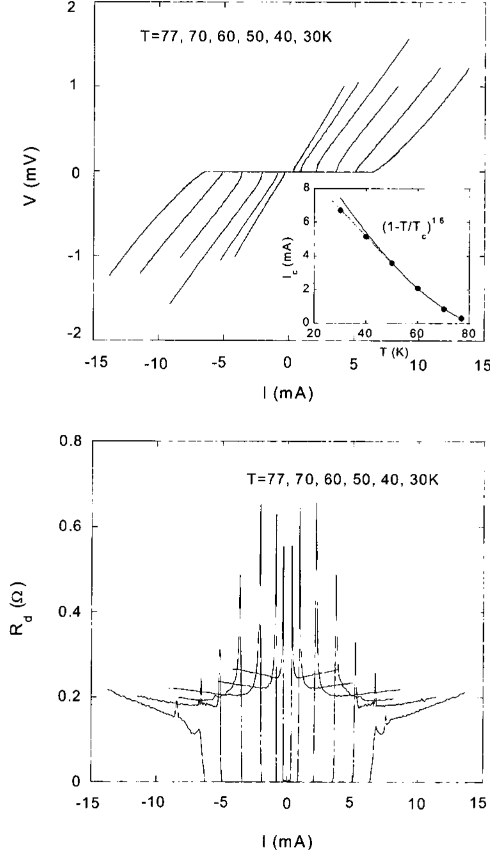


Fig. 2. *I-V* and the dynamic resistance $R_d$ (=d*V*/d*I*) curves from 30 to 77 K. All curves show RSJ-like behavior except 30 K where flux flow behavior sets in. The temperature dependence of $I_c$ is plotted in the inset. The solid line is a fit of $I_c$ for $T > 50$ K to $(1-T/T_c)^{1.6}$.

characteristics in Fig. 2. $R_n$ slightly decreases with temperature from 0.26 Ω at 77 K to 0.19 Ω at 30 K.

Fig. 2 shows the *I-V* and the dynamic resistance $R_d$ (=d*V*/d*I*) curves from 30 to 77 K. All curves show resistively-shunted-junction (RSJ) like behavior except 30 K where flux flow behavior sets in. The 60 K curve most resembles the ideal RSJ type as it exhibits the highest $R_d$. The temperature dependence of $I_c$ is plotted in the inset. The solid line is a fit of $I_c$ to $(1-T/T_c)^{1.6}$ for $T > 50$ K. For $T < 50$ K, $I_c$ increases linearly with lowering temperature. The exponent 1.6 is in between two typical barrier types, 1 for insulating and 2 for normal barrier. [8] Hence we can assume that the nature of the present barrier is a mixture of two types. The junction also shows large

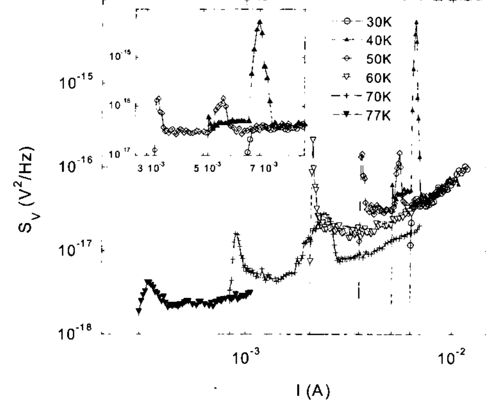


Fig. 3. The noise power spectral density $S_V$ as a function of current at 10 Hz. The inset is an expanded view of low-temperature $S_V$.

excess currents.

Fig. 3 shows the noise power spectral density $S_V$ at 10 Hz as a function of bias current $I_b$ at various temperatures. The inset shows the low temperature part for clarity. $S_V$ shows a peak at $I_b = I_c$ and increases with $I_b$. But in some temperatures additional peaks are observable at $I_b > I_c$. $S_V(I_c)$ is not monotonically dependent on temperature. It becomes maximal at 60 K where the largest $R_d$ is observed.

According to the RSJ model, we have $V = R_n (I_b^2 - I_c^2)^{1/2}$ and the voltage fluctuations can be expressed as $\delta V = (\partial V/\partial I_c)\ \delta I_c + (\partial V/\partial R_n)\ \delta R_n$, where $\delta I_c$ and $\delta R_n$ are fluctuations in and $R_n$, respectively. [3] Then the voltage-noise spectral density can be given as

$$S_V(f) = (V - R_d I)^2 S_I(f) + V^2 S_R(f) + k(V - R_d I) V S_{IR}(f) \tag{1}$$

Here, $S_I = |\delta I_c/I_c|^2$ and $S_R = |\delta R_n/R_n|^2$, and $S_{IR} = |\delta I_c/I_c||\delta R_n/R_n|$ is the cross-spectral density of the fluctuations, and $k$ is related to the correlation between $\delta I_c$ and $\delta R_n$. The normalized fluctuations $|\delta I_c/I_c|$ and $|\delta R_n/R_n|$ and $k$ are the fitting parameters to SV. For uncorrelated $\delta I_c$ and $\delta R_n$ fluctuations, we have $k$=0 while $k$=2 and –2 for inphase and antiphase correlated fluctuations. Fig. 4 shows the fitting results of 50 and 60 K noise with $k$ = -2. Quite a good fit to Eq. (1) indicates that the main source of the voltage noise is $\delta I_c$ and $\delta R_n$ fluctuations and they are antiphase correlated. The normalized fluctuations

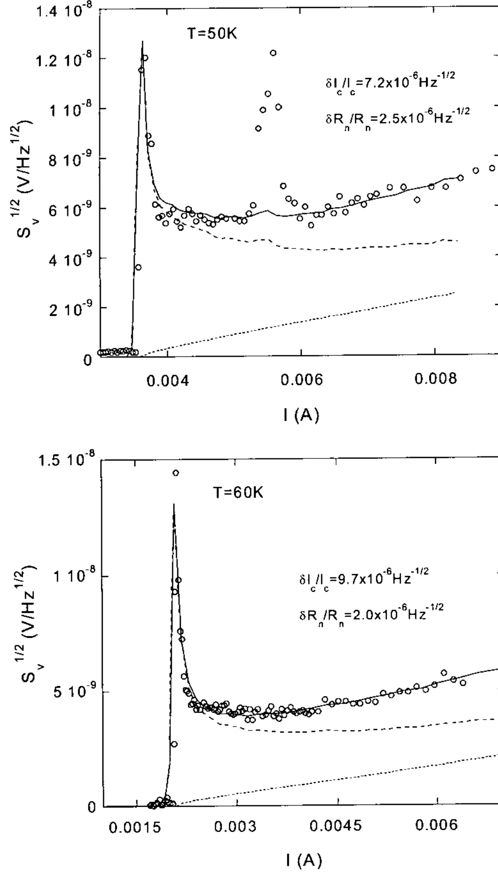


Fig. 4. Fitting result voltage noise $S_V^{1/2}$ to the RSJ model (solid line) at 50 and 60 K. The dotted line is the critical current fluctuations and the dashed line is the resistance fluctuations. An extra noise peak at 5.5 mA of 50 K is associated with a glitch in d$V$/d$I$ curves.

$|\delta I_c/I_c|$ and $|\delta R_n\ R_n|$ as a function of temperature are shown in Fig. 5. We find that $|\delta I_c/I_c| \sim 1.0\times10^{-5}$ Hz$^{-1/2}$ but slightly increasing with temperature and almost constant $|\delta R_n/R_n| \sim 2.0\times10^{-6}$ Hz$^{-1/2}$. The magnitude of $|\delta I_c/I_c|$ is similar to that of bicrystal junctions, but definitely smaller than other SNS-type ramp edge junction [4],[5]. One possible reason is that the columnar defects can reduce the magnetic flux noise of Josephson vortices by pinning provided by Abrikosov vortices in the YBCO electrodes.

Our findings are overall very similar to the results of Bi-2212 bicrystal grain-boundary junctions. There, a SIS model is adapted where the insulator is assumed to contain high density of localized states. [3] The pair current transferred by direct tunneling

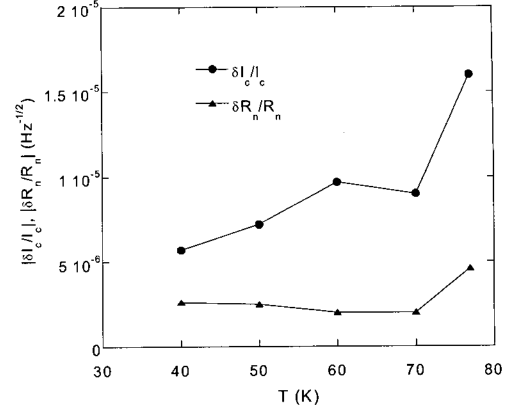


Fig. 5. The normalized fluctuations $|\delta I_c/I_c|$ and $|\delta R_n\ R_n|$ as a function of temperature are shown. The data are obtained from the fit shown in Fig. 4.

and the normal current is dominated by resonant tunneling via localized states inside the barrier. In this scheme, trapping and release of carriers in the localized states results in fluctuations of the barrier height. An increase of the barrier height causes a decrease of critical current and an increase of normal-state resistance. Therefore $\delta I_c$ and $\delta R_n$ fluctuations are expected to be antiphase correlated.

One peculiar feature of the noise power is the presence of an extra peak at $I_b > I_c$. The peaks are observed at 40, 50 and 70 K, but not in 60 and 77 K. The noise generally has a $1/f$ power spectrum, but at peaks we observed different frequency dependence at 40 and 50 K. In addition to that, one can clearly see in Fig. 4 that the extra peak is associated with a peak or glitch in the d$V$/d$I$ curves for 50 K. One can clearly see a d$V$/d$I$ peak at 40 K in Fig. 2 and corresponding huge noise peak in Fig. 3. A peak or glitch in the d$V$/d$I$ curves suggests that the transmission of the normal carriers is disturbed by some reason at a given bias current. During the disturbance, the transmission can be unstable and a large noise can be resulted due to such unstability.

A similar peak has been observed in some of YBCO/CRO/YBCO edge junctions at 4.2 K by Myers *et al.* [4]. They observed that the noise power spectrum is dominated by a single Lorentzian with the time trace showing a random telegraph signal. They interpreted the source of the telegraph noise is individual carrier trapped in the resistive channels. Since Myers *et al.* did not provide the corresponding

*IV* curves and, furthermore, $S_V$ at extra peaks were not Lorentzian in our experiments, a direct comparison cannot be made at present stage. A detailed study is further needed.

## III. Summary

We measured the transport properties of $YBa_2Cu_3O_x$ ramp-edge junctions fabricated with interface-engineered barrier and ion-irradiated thereafter. The current-voltage characteristics show a typical RSJ-like behavior. The analysis of the noise data using the RSJ model showed that the main source of the $1/f$ noise is the critical current and resistance fluctuations, and both fluctuations are antiphase correlated. The smaller magnitude of the critical current and resistance fluctuations compared with the previous studies seems to result from the columnar-defect induced effect.

## Acknowledgments

This work was financially supported by Yeungnam University Grant and Ministry of Science and Technology.

## References

[1] B. H. Moeckly and K. Char, "Properties of interface-engineered high $T_c$ Josephson junctions" Appl. Phys. Lett., 71, 2526-2528 (1997).

[2] M. Kawasaki, P. Chaudhari, and A. Gupta, "$1/f$ noise in $YBa_2Cu_3O_{7-\delta}$ superconducting bicrystal grain-boundary junctions" Phys. Rev. Lett., 68, 1065-1068 (1992).

[3] Marx, U. Fath, W. Ludwig, R. Gross, and T. Amrein, "$1/f$ noise in $Bi_2Sr_2CaCu_2O_{8+x}$ bicrystal grain-boundary Josephson junctions" Phys. Rev. B51, 6735-6738 (1995).

[4] K. E. Myers, K. Char, M. S. Colclough, and T. H. Geballe, "Noise characteristics of $YBa_2Cu_3O_{7-\delta}$ /CaRuO3/$YBa_2Cu_3O_{7-\delta}$ Josephson junctions" Appl. Phys. Lett., 64, 788-790 (1994).

[5] A. Flett, M. S. Colclough, Y. He, C. M. Muirhead, and R. A. Robinson, "Voltage-current characteristics and noise properties of SNS junctions" IEEE Transactions on Appl. Supercond., 5, 2973-2975 (1995).

[6] Gun Yong Sung and JunHo Kim, "Fabrication of interface-controlled Josephson junctions using $Sr_2AlTaO_6$ insulating layers" IEEE Transactions on Appl. Supercond., 11, 151-154 (2001).

[7] D. H. Kim, C. W. Lee, T. W. Lee, H. G. Hwang, G. Y. Sung, C. H. Choi, and T. S. Hahn, "Effect of columnar defects in $YBa_2Cu_3O_{7-x}$ ramp-edge Josephson junctions", Appl. Phys. Lett., 77, 3239-3241 (2000).

[8] A. Barone and G. Paterno, Physics and Applications of the Josephson Effect, John Wiley & Sons (1982).